Separation of Incident and Reflected Waves by Means of a Wave Radar System

Francesco Serafino, Simone Bonamano, Francesco Paladini de Mendoza, and Marco Marcelli

***Abstract*— This letter describes the wave reflection induced by the breakwater of the Port of Civitavecchia in the Tyrrhenian Sea, Italy, using a *X*-band wave radar. The wave radar system detected a complex structure of reflected waves that is composed of three spectral components and was generated by the complex structure of the breakwater. By applying a filter in the ω-k domain, it was possible to filter out the component of the incident waves to analyze the total component of reflected waves. Applying specific filters also made it possible to separate the spectral components of the single reflected waves. Bandpass filters were built to select each spectral component based on only the direction of the incident and reflected wave components. Starting from the separated spectral components, the reflection coefficients related to the measurement campaign were estimated and compared with the theoretical coefficients. The results confirm the potential of a radar system to resolve a complex sea state and provide a synoptic analysis of wave propagation processes over a wide measurement domain. Furthermore, this letter opens the way for new studies on the interaction between incident waves and coastal infrastructure.**

***Index Terms*— Radar, reflection, sea state, sea waves, waves.**

I. Introduction

WAVES that encounter emerged structures undergo multiple processes, including transmission and reflection. Wave reflection is among the most important factors that affect the hydrodynamics and sediment dynamics adjacent to structures. The reflected waves interfere with the incoming wave train and increase the wave activity in front of the structure. Knowledge of the hydrodynamic and morpho-dynamic processes induced by reflection has fundamental impacts on structural stability and ship navigation near harbors.

Since the 1950s, scientists have been working to increase the understanding of the interactions between waves and infrastructure for engineering practice. Several experiments have been conducted to separate the reflected wave parameters from the incoming wave parameters, which can be used for the accurate estimation of structure absorption and the hydrodynamic and morpho-dynamic effects [1]–[9]. Experiments have mainly been conducted in flumes, but field experiments have been poor and require great operational efforts and costs [2], [5], [9], [10].

Together with experiments, several empirical formulae have been developed for the prediction of the reflection coefficient for different kinds of structures using bathymetry and wave field analysis [1]–[4]. Most of these experiments were conducted in flumes, where waves propagate perpendicularly over a horizontal bed [5]–[10]. More recently, experiments have been conducted using a sloping bed, complex bathymetry, and oblique wave incidence [11], [12]. The data suggest that the effect of the sloping bottom and shoaling must be considered to improve the accuracy of reflection estimates.

As part of an experiment conducted in Monterey Bay, Dickson *et al.* [13] developed a new technique for reflection estimation, but it was limited to a directional spreading of 30° relative to the normal wave incidence. Since 1980, synthetic aperture radar (SAR) images have been used to estimate the sea state [14], and in late 1985, the research was extended to marine radar (*X*-band), which allows for analyses of the spatial and temporal evolution of the sea surface. *X*-band radar systems have operational flexibility, small dimensions, and low weight. Furthermore, they are easy to install on both movable and fixed stations to scan the sea surface with high temporal and spatial resolutions [15] for the spatial–temporal characterization of waves [16], [17]. The system has a wide range of applications in coastal monitoring and can detect a reflected component of the sea state [18], [19]. In these works, a secondary spectral component produced by a single reflected signal has been detected.

In this letter, we present the results of a radar survey of the complex breakwater of the Port of Civitavecchia, Italy, which was conducted during a storm. In recent decades, the Port of Civitavecchia has been greatly expanded and has become a nodal point for commercial and passenger ships. The extension of the Cristoforo Colombo breakwater has been carried out in multiple phases since 1990 and is ongoing, reaching a current length of 3.4 km. The different sections are designed in different ways, which result in different shapes, structures, and orientations. Thus, the sea state is determined by the interaction of incident waves with the complex breakwater. The spectral analysis of *X*-band radar data has allowed us to separate the reflected components by incident waves to reconstruct the 3-D space–time wave elevation of only reflected waves. The total composition of the reflected waves was also separated into individual reflected components generated by the complex breakwater structure.

This letter is organized as follows. The first section presents the characteristics of the study site, and the second section describes the methods used for the measurement campaign and

Manuscript received October 5, 2020; revised November 3, 2020 and November 19, 2020; accepted November 20, 2020. Date of publication February 2, 2021; date of current version December 17, 2021. This work was supported by the Civitavecchia Port Authority, which is a contribution to the Environmental Monitoring Project in the coastal marine area of Civitavecchia (Addendum 2). *(Corresponding author: Francesco Serafino.)*

Francesco Serafino is with the Institute for the Bioeconomy (IBE), National Research Council (CNR), 50127 Florence, Italy (e-mail: francesco.serafino@cnr.it).

Simone Bonamano and Marco Marcelli are with the Laboratory of Experimental Oceanology and Marine Ecology, Department of Ecology and Biology, University of Tuscia, 00053 Civitavecchia, Italy (e-mail: simo_bonamano@unitus.it; marcomarcell@unitus.it).

Francesco Paladini de Mendoza is with the Ente Fauna Marina Mediterranea, 96012 Avola, Italy (e-mail: framendoza1985@gmail.com).

This article has supplementary downloadable material available at https://doi.org/10.1109/LGRS.2021.3050829, provided by the authors.

Digital Object Identifier 10.1109/LGRS.2021.3050829

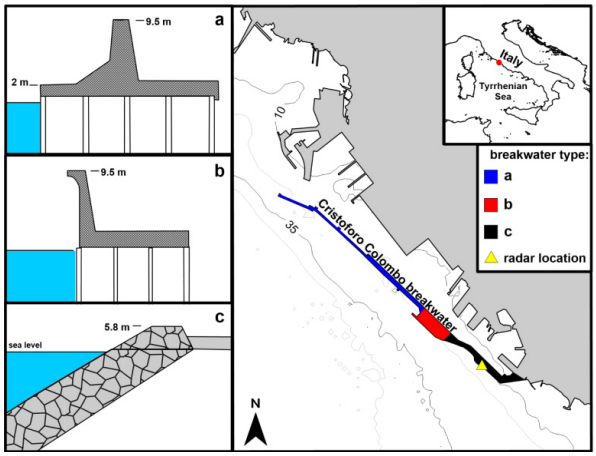

Fig. 1. Study area. Different colors indicate the different structures (a,b,c) that form the Cristoforo Colombo breakwater. The yellow triangle shows the position of the radar system. In the square on the top right side, the red circle indicates the location of Civitavecchia along the Italian coast.

radar image processing. The third section presents an analysis of the radar measurements that allowed us to describe the wave reflection process upon the long composite breakwater of the Port of Civitavecchia. The study highlights the ability of the radar system to resolve the complex sea state and to provide a useful tool for in-field, real-time wave reflection monitoring.

II. Study Area

The Port of Civitavecchia is located on the central western coast of Italy (Fig. 1).With planned structural changes, the port is set to become one of the largest ports of the Mediterranean Sea. In the current configuration, the harbor is 3.3 km long and 500-m wide. The surrounding coastal area is characterized by a rocky shore with mild slope, which includes several human-made structures, such as the pier of a coal-fired power plant in the north and beach protection barriers in the south. The water depth in front of the Cristoforo Colombo breakwater ranges from 25 to 30 m, and the slope of the seabed varies between 1.3% and 2.2%.

The breakwater is characterized by three distinct structures (Fig. 1). The cross section in panel *a* of Fig. 1 was completed recently (2015). It is composed of plain vertical wall caissons up to 2 m above sea level (relative to the seaward edge of the caisson) and a backward-located straight parapet wall that reaches a height of 9.5 m above sea level. The toe of the caissons is located at −22 m beyond the sea level, where two layers of quarry stone berm form a foot protection for the caisson foundation.

This structure is 2 km long and is composed of two sections with different orientation. The northern section is 500 m long and oriented west-north-west to east-south-east, while the southern section is 1.5 km long and oriented north-west to south-east. The cross section in panel *b* of Fig. 1 extends for 500 m and is the result of renovation works that ended in 2011. It is composed of a plain vertical wall caisson and a recurved parapet wall that is aligned to the seaward caisson edge with the same height as cross section *a*.

The toe of the caissons in this section is located at 12 m, where two layers of quarry stone berm form the foot protection for the caisson foundation. The cross section in panel *c* of Fig. 1 is the oldest breakwater of the port. It is characterized by a quarry stone mound that extends for 1 km and a slope of 50%. It is protected with 25-ton tetrapods.

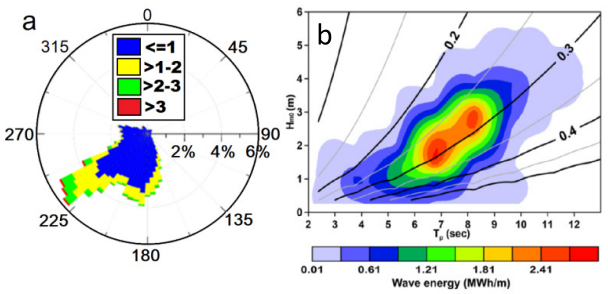

Fig. 2. Wave conditions based on 15-year time-series records. (a) Directional distribution of waves (colors indicate significant wave height expressed in meters). (b) Diagram of reflection coefficients (Kr) computed using a formula from Isaacson *et al.* [5] represented by contour lines overlapped with the distribution of total annual energy per meter of the wavefront (colored contour).

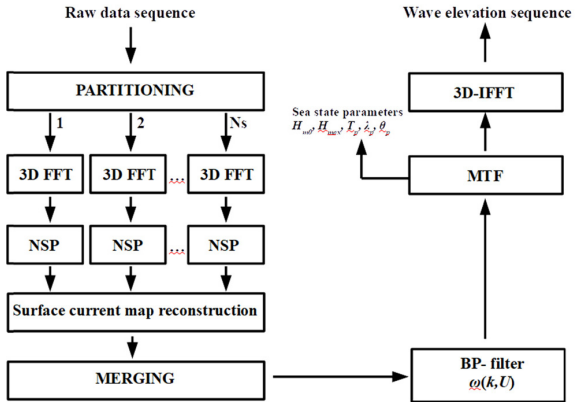

Fig. 3. Block diagram of radar image processing.

The wave climate [Fig. 2(a)] was recorded by a wave buoy that is part of the Civitavecchia Coastal Environment Monitoring System (C-CEMS) [20]. Waves predominantly come from the south-west (232° ± 15°N) and south (182° ± 20°N). The waves impact the breakwater with an average incidence angle of 6° for waves coming from the southwest and of about 44° for waves coming from the south. Mendoza *et al.* [21] estimated the available offshore wave energy in the area of Civitavecchia [Fig. 2(b)]. Their analysis indicated an average annual energy of 31.68 MW/h, which is subject to seasonal oscillation with the maximum value occurring during the winter and fall seasons. The most energetic wave conditions occur for the events with H_{m0}(significant wave height) between 1.5 and 3 m and Tp (peak period) within 6–9 s. The storm event analyzed in this letter is included in these ranges ($H_{m0} = 1.5$ and $T\text{p} = 6.6$) and comes from the southwest (235 °N), which corresponds to the predominant and prevailing wave direction.

III. Wave Radar System

The raw radar data processing follows a methodology that was fully explained by Serafino *et al.* [16] and consists of five main steps, which are summarized in Fig. 3.In the first step, the radar image sequence is transformed into a 3-D image spectrum using a 3-D-Fast Fourier Transform (3-D-FFT). Next, the effect of the received signal power decay along the range direction, which has smaller variability than the effect associated with the phase of the signal, is filtered by applying a high-pass (HP) filter to the image spectrum $F_I(k_x, k_y, \omega)$ [22].

In the second step, the linear gravity wave components are extracted from the image spectrum $F_I(k_x, k_y, \omega)$. The filtering exploits the dispersion relation relating the wavenumber ($\bar{k}$) to the angular frequency (ω) through the sea surface current

$\overline{U} = (U_x, U_y)$ and the water depth h. The dispersion relation is expressed as

$$\omega(\overline{k}) = \sqrt{g|\overline{k}|\tanh(|\overline{k}|h)} + \overline{kU} \tag{1}$$

where g is the acceleration due to gravity at the Earth's surface, and k is

$$k = |\overline{k}| = \sqrt{k_x^2 + k_y^2}. \tag{2}$$

The current vector $\overline{U} = (U_x, U_y)$ needs to be estimated before applying the dispersion relation [15]. For this purpose, the third step involves a methodology based on the maximization of the normalized scalar product (NSP), which was developed by Serafino *et al.* [16] Once the current $\overline{U} = (U_x, U_y)$ has been estimated, it is possible to build the bandpass (BP) filter $G(k_x, k_y, \omega, U_x, U_y)$ based on (1) and apply it to the image spectrum $F_I(k_x, k_y, \omega)$ (see the block diagram in Fig. 3). The result of this procedure is the function $\check{F}_I(k_x, k_y, \omega)$.

The fourth step is to move from the filtered image spectrum $\check{F}_I(k_x, k_y, \omega)$ to the desired sea-wave spectrum $F_W(k_x, k_y, \omega)$ by minimizing the effects of modulation phenomena. This step could be implemented using a modulation transfer function (MTF) that allows the transformation from the radar spectrum to the sea spectrum

$$F_w(k_x, k_y, \omega) = \frac{\check{F}_I(k_x, k_y, \omega)}{|M(k)|^2} \tag{3}$$

where $|M(k)|^2 = k^\beta$ is the MTF.

A previous empirical analysis found a good estimation with $\beta = -1.2$ [22]. When the wave spectrum $F_w(k_x, k_y, \omega)$ is determined, it is possible to extract some parameters about the sea state. This is performed by generating a wavenumber directional spectrum, of which the maximum provides the wavelength and propagation direction (λ_p, ϑ_p) of the primary wave. The last step provides the evolution of the wave height $\eta(x, y, t)$ by performing an inverse 3-D FFT on the function $F_w(k_x, k_y, \omega)$. Starting from the total directional spectrum, the spectral components of the wave spectrum have been isolated by a filter BP [22]. The time–space evolution of waves and the statistical parameters have been reconstructed for the whole sea state and the incident and reflected wave components.

IV. Measurement Campaign

The wave radar system was a *Marine Sperry X*-band radar, which was installed for 1 day during a summer storm on July 27, 2015, at 12:00 UTC, along the Cristoforo Colombo breakwater of the Port of Civitavecchia. The radar system radiates a maximum power of 25 kW and is equipped with an 8-foot (2.4 m) antenna. The radar antenna was located at coordinates of Lat. 42° 05'26.53"N and Lon. 11° 47'5.85"E.

The antenna was installed on a terrace of an old pilots building at a height of 10 m above sea level. The details of the data-acquisition parameters are as follows: Radar scale = 1.23 NM; Antenna rotation period (Δt) = 194 s; Spatial image spacing (Δx and Δy) = 4.4 m; Antenna height = 10 m; and View angular sector = 160°N. The wave condition during the acquisition never changes in terms of intensity and direction. Fig. 4 shows a radar image that was collected during the storm, in which the sea wave pattern can be seen. The intersection of black lines indicates the location of the radar.

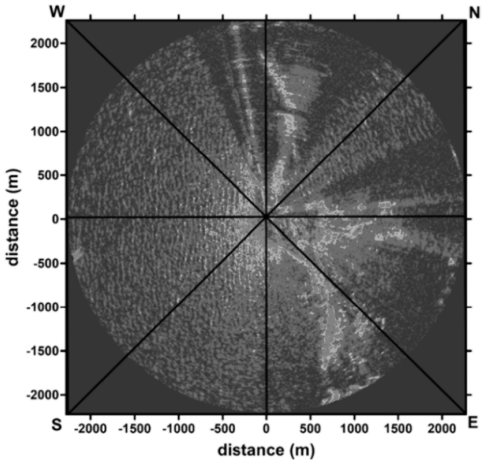

Fig. 4. A radar image collected during a storm. The intersection of the black lines indicates the position of the radar.

V. Wave Reflection in Design Condition

During the project design phases of the Cristoforo Colombo breakwater, the reflection coefficient (*Kr*) was estimated based on laboratory experiments. In particular, for cross sections *a* and *b* in Fig. 1, laboratory experiments were conducted using a 2-D-Froude Model-scaled model (1:35) located at the Laboratorio di IdraulicaAmbientale e Marittima (LIAM) of the University of Aquila [23]. The results of these experiments were used for the executive projects of the Cristoforo Colombo breakwater to determine the stability of the caisson design and the overtopping performance. Section *c* is the oldest structure of the Port of Civitavecchia and was built before 1980, so the predicted *Kr* value was not available. This problem was solved by applying the empirical formulation developed by Zannutigh *et al.* [4], which is suitable for all kinds of revetment materials, considering the roughness factor of armor units and the breaking index.

The breaking index (or Iribarren–Battjes parameter, $\xi 0$) is defined as a dimensional ratio between the beach slope (or structure slope) and the steepness of waves

$$\xi 0 = \frac{\tan(\alpha)}{\frac{\sqrt{2\pi H_m^0}}{gT_m^2}} \tag{4}$$

where α is the beach (or structure) slope, g is the gravitational acceleration, H_{m0} is the significant wave height at the structure toe, and T_m is defined for single peak wave spectra as $T_m = T_p/1.1$, where T_p is the peak period of incident waves. The breaking index describes the breaking process, which causes energy dissipation, thus making it a fundamental parameter in the evaluation of energy loss when the waves are breaking on a structure. The formula developed by Zannutigh *et al.* [4] depends on the breaking index (ξ_0) and two coefficients (a, b) according to the following relation:

$$Kr = \tanh\left(a\xi_0^b\right) \tag{5}$$

where the two coefficients are calculated from the following equations:

$$a = 0.167\left[1 - \exp(-3.2\gamma f)\right] \tag{6}$$

$$b = 1.49(\gamma f - 0.38)^2 + 0.86 \tag{7}$$

where γ_f is the roughness coefficient of the armor unit. A γ_f value of 0.38 is applied for the armor unit consisting of tetrapods [24].

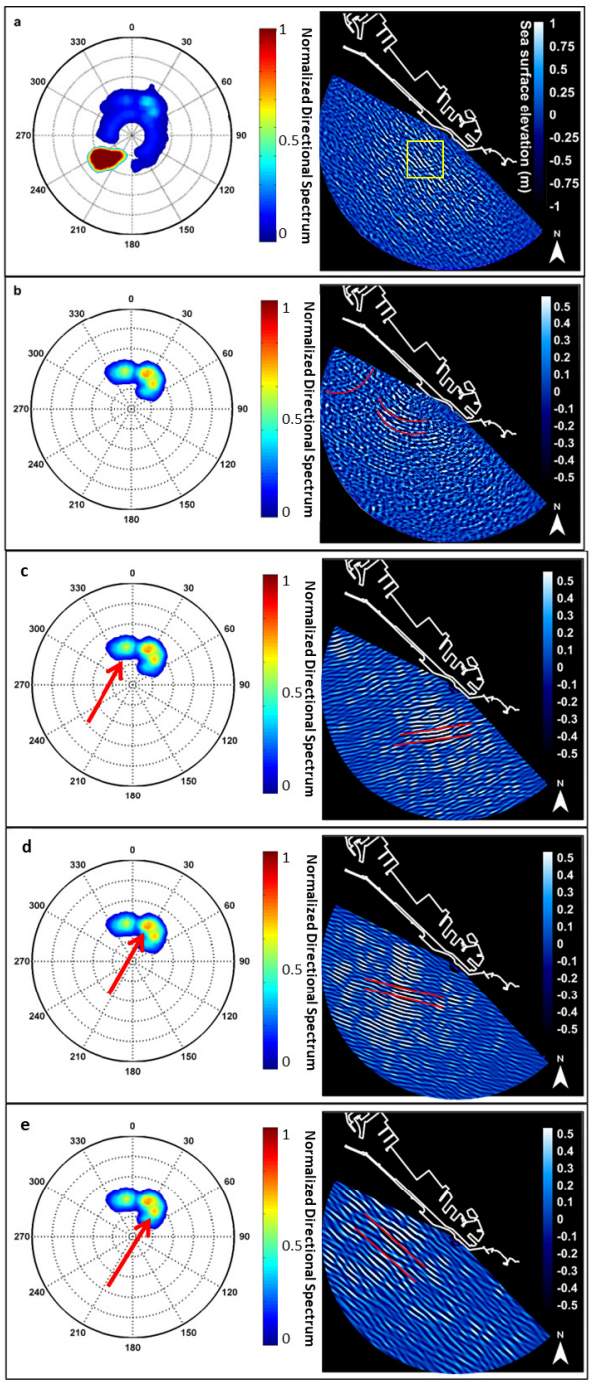

Fig. 5. Directional spectrum obtained from the Remocean system records. (a) Directional wave spectra and 3-D surface elevation of the full sea state. (b) Directional wave spectra and 3-D surface elevation of total reflected wave field obtained by filtering out the incident wave component. The red line on the 3-D surface emphasizes the curve wavefronts propagating in the offshore direction. (c)–(e) Directional wave spectra and 3-D surface elevation of every component of the reflected wave field. The *red arrows* on the directional wave spectra indicate the spectral component reconstructed in 3-D.

VI. Results

The directional wave spectra obtained by the full radar records (Fig. 5) highlights the presence of multiple wavenumber peaks, where the highest peak corresponds to the incident waves coming from about 232°N. The three lower peaks with different intensities and directions correspond to the total reflected component. Likewise, on the 3-D surface elevation, the reflected waves overlap with the well-defined incident

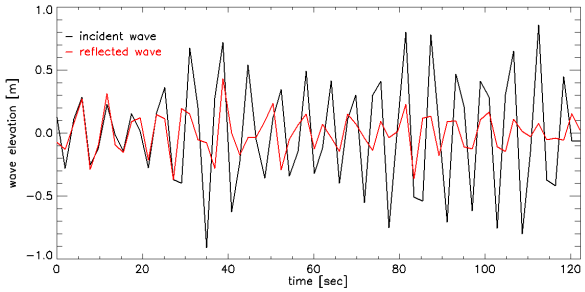

Fig. 6. Plot of the wave elevation over time at a point located in the center of the subarea (*yellow square*) in Fig. 5. Right side for the only incident and reflected wave components.

wave trains propagating to the shore, and the alignment is quite parallel.

We obtained the total reflected component by applying a BP filter in the ω-k domain to filter out the incident waves. The total reflected component is composed of three well-defined peaks with different intensities and orientations. The reconstruction of the 3-D surface elevation obtained by applying the inverse FFT to the filter 3-D spectrum highlights curved (circular) reflected wavefronts propagating offshore in different directions [Fig. 5(b)]. Starting from the total reflected spectral component [Fig. 5(b), left], three spectral filters were applied to separate the three different reflected components that are visible in the same figure and indicated by *red arrows* in Fig. 5(c)–(e).The reason is the complex breakwater structure, which reflects the incident waves in different directions.

The three spectral filters have been built manually by selecting, for each reflected component, the portion of the spectrum that includes the spectral components from the spectral peak to 10% (chosen empirically) of its value. In the future, more accurate procedures will be examined for the automatic separation of various spectral components. The result of the filtering procedure is three different nearly plane waves with different directions and periods due to the different behaviors of the three parts of the dam, as expected from the wave theory. Its composition generates the circular waves shown on the right side of Fig. 5(b).

The reflection coefficient related to these specific incident wave conditions can be evaluated by considering the ratio between the spectral power of the reflected wave and incident wave. Considering the total reflected spectral component, the reflection coefficient extending over the total radar domain is 0.43. To better analyze the effect of the wave reflection closer to the dam, we also estimated the reflection coefficient in a limited domain, which is indicated by the *yellow square* in Fig. 5(a) (right). In this subarea, the reflection coefficient is 0.5. Fig. 6 shows a plot of the wave elevation over time at a point located in the center of the subarea for the only incident wave (where the reflected waves have been filtered out) and for the component of the reflected wave.

Table I shows the statistical parameters derived from the total sea state and incident and total reflected spectral components. To validate the methods used to analyze the sea state through the wave radar system, the incident wave parameters were compared with those provided by the ECMWF and are: $H_{m0} = 0.9$ m; $T_p = 6.3$ s; and $Dp = 239$°N. Based on the wave conditions of the study area (Fig. 2), Kr values between 0.2 and 0.5 are highlighted in the analysis of the reflection coefficient for breakwater type c using the formulation of Zannutigh *et al.* [4] [Fig. 2(a)].

TABLE I

STATISTICAL PARAMETERS OBTAINED BY WAVE RECORDS FOR THE TOTAL SEA STATE AND FOR EACH SPECTRAL COMPONENT

Type	H_{m0} (m)	T_p (s)	Dp (°N)	Dm (°N)	Dir spread (°N)
Total wave field	1.2	6.5	232	230	180
Incident wave	1.0	6.5	232	230	9
Reflected waves	0,6	6.5	25	16	55

The estimated Kr for section $c = 0.26$, relative to the conditions that occurred during the radar survey, and the Kr for other sections obtained from the technical documentation of the Port Authority based on model experiments [23] are: a (for $H_{m0} < 2$ m) $= 0.80$; a (for $H_{m0} > 2$ m) $= 0.58$; and $b = 0.80$. Regarding breakwater type a, two distinct Kr values are available depending on the height of incident waves. Until the first step of cross section a (up to 2 m high), the breakwater is like a section with a vertical wall but with a slope change of more than 2 m.

The differences between the Kr index estimated by the radar and by the Zannutigh equation might be due to several factors. The most relevant one is due to the complex structure of the breakwater, which generates more complex reflection with respect to that considered in the Zannutigh model. In particular, the Kr index estimated by the radar is affected by the reflection of both types a and b.

VII. CONCLUSION

This letter has described the wave reflection induced by the breakwater of the Port of Civitavecchia through the use of X-band wave radar. The analysis of wave radar records allowed for the separation of the spectral components of the total wave field and the reconstruction of the 3-D sea surface elevation induced by each reflected component. The wave conditions chosen for the radar measurements are close to the most energetic events of the study area.

The 3-D surface reconstruction of the total reflected waves highlights the presence of curved wavefronts propagating in south-eastward and south-westward directions. The reflected waves have a finite length along their crest line that depends on the extension of the reflective source. Furthermore, they disperse during propagation away from the source of reflection. The superposition of the three single plane waves reflected by the dam structure generates a circular wavefield that propagates offshore. The reflection coefficient measured by the radar data was compared with the theoretical coefficient provided by the empirical formulation developed by Zannutigh *et al.* [4], which does not take into account the mutual interaction of the different parts of the port structure.

It is important to emphasize that the results presented refer to the analysis of data acquired from 1 h of radar measurements. The results confirm the potential of a radar system to resolve a complex sea state and provide a synoptic analysis of the wave propagation processes over a wide measurement domain. However, it did not allow for a complete analysis of the reflection caused by the complex port structure. A complete analysis would require measurement data from various sea conditions, including the height, direction, and period of incident waves, to be able to carry out an exhaustive characterization of the reflection coefficients. BP filters were built to select each spectral component based on only the direction of the incident and reflected wave components. In future work, we will develop more sophisticated approaches to separate incoming and reflected waves.

REFERENCES

[1] M. Miche, "Le pouvoir réfléchissant des ouvrages maritimes exposés à l'action de la Houle," *Ann. PontsChausées*, vol. 121, pp. 285–319, Apr. 1951.

[2] W. N. Seelig and J. P. Ahrens, "Estimation of wave reflection and energydissipation coefficients for beaches, revetments and breakwaters," CERC, New Delhi, India, Tech. Rep. 81-1, 1981.

[3] M. A. Davidson, P. A. D. Bird, G. N. Bullock, and D. A. Huntley, "A new non-dimensional number for the analysis of wave reflection from rubble mound breakwaters," *Coastal Eng.*, vol. 28, nos. 1–4, pp. 93–120, Sep. 1996.

[4] B. Zanuttigh and J. W. van der Meer, "Wave reflection from coastal structures in design conditions," *Coastal Eng.*, vol. 55, no. 10, pp. 771–779, Oct. 2008.

[5] M. Isaacson, "Measurement of regular wave reflection," *J. Waterway, Port, Coastal, Ocean Eng.*, vol. 117, no. 6, pp. 553–569, Nov. 1991.

[6] P. Frigaard and M. Brorsen, "A time-domain method for separating incident and reflected irregular waves," *Coastal Eng.*, vol. 24, nos. 3–4, pp. 205–215, Mar. 1995.

[7] A. Baquerizo, M. A. Lasoda, J. M. Smith, and N. Kobayashi, "Cross-shore variation of wave refection from beaches," *J. Waterway, Port, Coastal Ocean Eng.*, vol. 123, pp. 274–279, Dec. 1997.

[8] J. R. Medina, "Estimation of incident and reflected waves using simulated annealing," *J. Waterway, Port, Coastal, Ocean Eng.*, vol. 127, no. 4, pp. 213–221, Aug. 2001.

[9] K. D. Suh, W. S. Park, and B. S. Park, "Separation of incident and reflected waves in wave–current flumes," *Coastal Eng.*, vol. 43, nos. 3–4, pp. 149–159, Aug. 2001.

[10] D. A. Huntley, D. Simmonds, and R. Tatavarti, "Use of collocated sensors to measure coastal wave reflection," *J. Waterway, Port, Coastal, Ocean Eng.*, vol. 125, no. 1, pp. 46–52, Jan. 1999.

[11] T. E. Baldock and D. J. Simmonds, "Separation of incident and reflected waves over sloping bathymetry," *Coastal Eng.*, vol. 38, no. 3, pp. 167–176, Nov. 1999.

[12] H.-K. Chang and T.-W. Hsu, "A two-point method for estimating wave reflection over a sloping beach," *Ocean Eng.*, vol. 30, no. 14, pp. 1833–1847, Oct. 2003.

[13] W. S. Dickson, T. H. C. Herbers, and E. B. Thornton, "Wave reflection from breakwater," *J. Waterway, Port, Coastal, Ocean Eng.*, vol. 121, no. 5, pp. 262–268, Sep. 1995.

[14] S. Hasselmann, C. Bráning, K. Hasselmann, and P. Heimbach, "An improved algorithm for the retrieval of ocean wave spectra from synthetic aperture radar image spectra," *J. Geophys. Res., Oceans*, vol. 101, no. C7, pp. 16615–16629, Jul. 1996.

[15] I. R. Young, W. Rosenthal, and F. Ziemer, "Three-dimensional analysis ofmarineradarimagesforthedeterminationofoceanwavedirectionality and surface currents," *J. Geophys. Res.*, vol. 90, no. 1, pp. 1049–1059, 1985.

[16] F. Serafino, C. Lugni, and F. Soldovieri, "A novel strategy for the surface current determination from marine X-band radar data," *IEEE Geosci. Remote Sens. Lett.*, vol. 7, no. 2, pp. 231–235, Apr. 2010.

[17] F. Serafino *et al.*, "REMOCEAN: A flexible X-band radar system for sea-state monitoring and surface current estimation," *IEEE Geosci. Remote Sens. Lett.*, vol. 9, no. 5, pp. 822–826, Sep. 2012.

[18] G. Ludeno *et al.*, "Remocean system for the detection of the reflected waves from the costa concordia ship wreck," *IEEE J. Sel. Topics Appl. Earth Observ. Remote Sens.*, vol. 7, no. 7, pp. 3011–3018, Jul. 2014.

[19] G. Ludeno *et al.*, "An X-band radar system for bathymetry and wave field analysis in a Harbour area," *Sensors*, vol. 15, pp. 1691–1707, Jan. 2015.

[20] S. Bonamano *et al.*, "The Civitavecchia coastal environment monitoring system (C-CEMS): A new tool to analyze the conflicts between coastal pressures and sensitivity areas," *Ocean Sci.*, vol. 12, no. 1, pp. 87–100, Jan. 2016.

[21] F. Paladini de Mendoza *et al.*, "Where is the best site for wave energy exploitation? Case study along the coast of northern Latium (ITALY)," *J. Coastal Conservation*, vol. 20, no. 1, pp. 13–29, Feb. 2016.

[22] J. Nieto Borge, G. R. RodrÌguez, K. Hessner, and P. I. González, "Inversion of marine radar images for surface wave analysis," *J. Atmos. Ocean. Technol.*, vol. 21, no. 8, pp. 1291–1300, Aug. 2004.

[23] R. M. Di, G. M. Beltrami, and G. P. De, "Laboratory investigation on wave overtopping of composite breakwaters: The port of Civitavecchia case," *Coastal Eng.*, vol. 1, pp. 4616–4627, Dec. 2006.

[24] T. Bruce, J. van der Meer, L. Franco, and J. M. Pearson, "A comparison of overtopping performance of different rubble mound breakwater armour," in *Proc. Coastal Eng.*, San Diego, CA, USA, Apr. 2007, pp. 4567–4579.